Available online at ScienceDirect

ScienceDirect

J. Mater. Sci. Technol., 2015, 31(1), 37−42

Influence of Substrate Negative Bias on Structure and Properties of TiN Coatings Prepared by Hybrid HIPIMS Method

Zhenyu Wang[1,2], *Dong Zhang*[1], *Peiling Ke*[1)*], *Xincai Liu*[2], *Aiying Wang*[1)**]

1) Key Laboratory of Marine Materials and Related Technologies, Zhejiang Key Laboratory of Marine Materials and Protective Technologies, Ningbo Institute of Materials Technology and Engineering, Chinese Academy of Sciences, Ningbo 315201, China

2) Faculty of Materials Science and Chemical Engineering, Ningbo University, Ningbo 315201, China

[Manuscript received December 4, 2013, in revised form March 1, 2014, Available online 8 July 2014]

TiN coatings were deposited using a hybrid home-made high power impulse magnetron sputtering (HIPIMS) technique at room temperature. The effects of substrate negative bias voltage on the deposition rate, composition, crystal structure, surface morphology, microstructure and mechanical properties were investigated. The results revealed that with the increase in bias voltage from −50 to −400 V, TiN coatings exhibited a trend of densification and the crystal structure gradually evolved from (111) orientation to (200) orientation. The growth rate decreased from about 12.2 nm to 7.8 nm per minute with the coating densification. When the bias voltage was −300 V, the minimum surface roughness value of 10.1 nm was obtained, and the hardness and Young's modulus of TiN coatings reached the maximum value of 17.4 GPa and 263.8 GPa, respectively. Meanwhile, the highest adhesion of 59 N was obtained between coating and substrate.

KEY WORDS: **TiN; Hybrid HIPIMS; Substrate bias; Microstructure; Mechanical properties**

1. Introduction

Due to the attractive properties such as high hardness, good wear resistance and chemical stability, TiN coatings as one of the protective hard coatings have received a wide range of applications in cutting tools, dies and many mechanical components to improve their lifetime and performance[1,2]. Since 1980s, many methods have been developed to prepare TiN coatings, typically the dc magnetron sputtering (dcMS) technique and cathodic arc ion plating (AIP)[3−5]. Even the dcMS technique is beneficial to depositing TiN coatings with smooth surface over large area, but the low ionization degree of used metal target is usually <5%[6], which causes the porous and loose column structure of the deposited TiN coatings. AIP process is characterized by a combination of high deposition rate and high ionization degree of the plasmas, but the co-deposition of macro-particles is the main barrier to obtain the high performance coatings with smooth surface[7]. Additionally, many efforts have been made by many researchers to improve the ionization of magnetron sputtering, such as the unbalanced magnetron sputtering[8], and plasma enhanced magnetron sputtering[9]. Up to now, new magnetron sputtering method called high power impulse magnetron sputtering (HIPIMS) (also known as high power pulsed magnetron sputtering (HPPMS)) by Kouznetsov et al.[10] and modulated pulsed power magnetron sputtering (MPPMS) by Chistyakov et al.[11] have been developed, respectively, which are aimed to obtain the high density plasma and high sputtering ionization ratio similar to those of AIP technique. The key process of these techniques is to apply a pulsed high peak target power density (e.g., 1−3 kW/cm^2 in HIPIMS, and 0.5−1.5 kW/cm^2 in MPPMS) on the target for a short running time (e.g., 100−500 μs in HIPIMS, and 500−3000 μs in MPPMS[12]). This pulsed peak power can be typically 100 times larger than that in the conventional magnetron sputtering power. Consequently, a high density plasma about 2−3 orders of magnitude higher than that obtained in conventional magnetron sputtering, and a high ionization degree of the sputtered material can be generated by the strong ionizing collisions between the sputtered atoms and energetic electrons[10,13].

However, HIPIMS requires higher excitation voltage, and then the ionized particles may be drawn back by target itself because

* Corresponding author. Ph.D; E-mail address: kepl@nimte.ac.cn (P. Ke).
** Corresponding author. Prof., Ph.D.; Tel.: +86 574 86685036; Fax: +86 574 86685159; E-mail address: aywang@nimte.ac.cn (A. Wang).
1005-0302/$ — see front matter Copyright © 2014, The editorial office of Journal of Materials Science & Technology. Published by Elsevier Limited. All rights reserved.
http://dx.doi.org/10.1016/j.jmst.2014.06.002

the high negative voltage occurred in the target surface, causing low coating deposition rate[14]. Therefore, the low deposition rate is now a major barrier to the commercial application of HIPIMS. To solve this problem, we developed a modified HIPIMS power supply coupled a dc unit with the high power pulse unit in the present work. The coupled dc unit not only can ensure a high deposition rate but also optimize pulse glowing and plasma stabilization through pre-ionization[15,16]. In addition, the high power pulse can produce plasmas with highly ionized metallic species occupying high ion energy.

Taking a much higher ratio of ion to neutral for the sputtered species into account, negative bias voltage may have a significant influence on the structure and properties of TiN coatings during HIPIMS process because of an intense and controllable bombardment of the coating growth with energetic ions from the sputtered target materials and the process gases, by varying the substrate bias[17]. In addition, during the HIPIMS deposition process, the deposition and properties of TiN coatings are still lack of understanding. In this work, we presented the deposition of TiN coatings by a home-made hybrid HIPIMS technique at room temperature, the effects of substrate negative bias voltage on the structure and properties of coatings were investigated.

2. Experimental

The TiN coatings were reactively magnetron sputtered in mixed Ar/N_2 precursor gases in a hybrid HIPIMS system as schematically shown in Fig. 1. The parallel connection of HIPIMS power supply was revealed in our previous study[14], in which the pulsed power by the constant voltage mode was adjusted to achieve the high impulse power and the dc power by the constant current mode ensured to obtain the high deposition rate and stable discharged plasma. The p-type Si (100) wafers, mirror-finished high speed steel (HSS) with a dimension of 15 mm × 15 mm × 3 mm and WHEEL BRAND glass pieces were used as the substrates, respectively. Before deposition, all the substrates were cleaned ultrasonically in acetone and ethanol each for 15 min and then dried in air. Thereafter, the substrates were fixed on a rotary sample holder with a distance of 16 cm to the sputtering target. The magnetron cathode equipped with a pure Ti target (400 mm × 100 mm × 7 mm, purity of 99.99%) was controlled with the hybrid pulsed high power supply. The chamber was first evacuated to a base pressure of lower than 3.99×10^{-3} Pa (3.0×10^{-5} Torr) and then the plasma etching was conducted by Ar glow discharge for 30 min. In order to improve the adhesion between the TiN coating and substrate, the

Table 1 Process parameters for TiN coatings deposition

Deposition parameters	Ti interlayer	TiN coatings
Ar (sccm)	50	50
N_2 (sccm)	0	10
Pulse width (μs)	200	200
Pulse frequency (Hz)	100	100
Pulse voltage (V)	600	600
DC current (A)	3.0	3.0
Negative bias voltage (V)	−300	−50, −100, −200, −300, −400
Deposition time (min)	15	80, 90, 100, 110, 120

Ti interlayer of about 230 ± 20 nm was deposited after the precleaning stage. During deposition, the reactive gas of N_2 was introduced into the chamber to form TiN coating. The thickness of the TiN coating was kept at about 900 ± 100 nm. The process parameters are illustrated in Table 1. As shown in Fig. 2, the peak voltage and current of Ti target were 510 V and 108 A, respectively. Substrate negative bias voltage from −50 to −400 V, with a frequency and duration of 350 kHz and 1.1 μs, was applied to the substrates and no external heating was provided during deposition.

The target current was evaluated by using a current monitor (LEM, Model LT58-S7) and the target voltage was tested with a voltage probe (Tektronix, model TPP0101). These in-situ waveforms during deposition were monitored with an oscilloscope (Tektronix, model TDS 1012C-SC). The thickness of the deposited coatings was measured with a surface profilometer (KLA-Tencor, Alpha-Step IQ) through a step between the coating and Si wafers covered with a shadow mask. Surface morphology and cross-section morphology of the coatings were observed by field emission scanning electron microscopy (S4800, Hitachi). Energy-dispersive X-ray spectroscopy (EDS) was used to gain insight into the chemical compositions. Quantification was performed using the ZAF method, which was incorporated with individual corrections from the atomic number (Z), absorption (A), and fluorescence (F). The surface roughness was evaluated with a scanning probe microscope (Dimension 3100V, Veeco, US) at a scan rate of 1.0 Hz. The average roughness (Ra) values of the coating surfaces was calculated from 512 × 512 surface height data points over 3 μm × 3 μm scan area. Structural analysis of the films was performed by X-ray diffraction (XRD) at ambient air using a Bruker D8 X-ray facility (Cu-$K\alpha$ radiation). Mechanical properties of the coatings were tested by the nano-indentation technique (MTS NANO

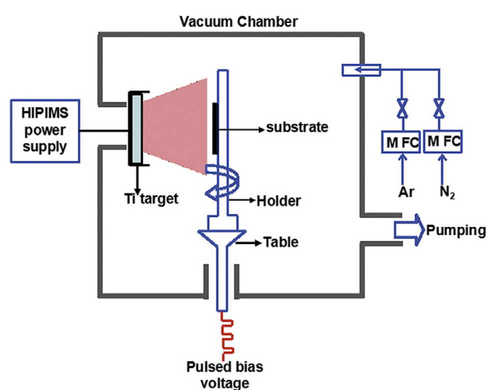

Fig. 1 Schematic diagrams of the hybrid HIPIMS deposition system of TiN coatings.

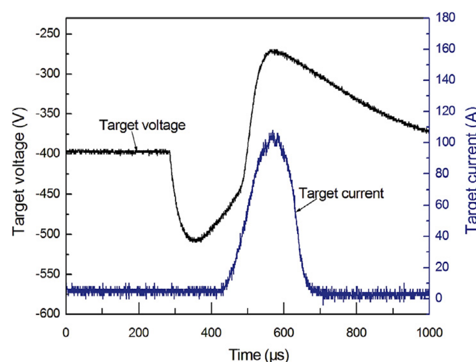

Fig. 2 Waveforms of the target voltage and target current at a pulsed period.

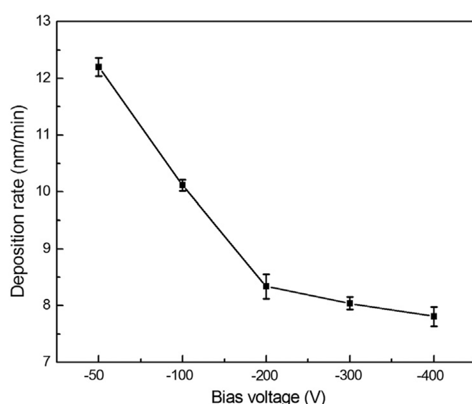

Fig. 3 Deposition rate of the coatings as a function of the bias voltage.

G200) in a continuous stiffness measurement mode using a Berkovich diamond tip. The characteristic hardness was chosen in a depth of around 1/10 of the coating thickness where the measured value was not affected by the Si substrate. Four replicate indentations were done for each sample. To assess coating adhesion, the critical loads, L_C, where the mass delamination of coating happens, were measured on the CSM Revetest scratch tester with a diamond tip of a radius of 200 μm, under a maximum load of 80 N and a scratch length of 3 mm.

3. Results and Discussion

The average growth rate of TiN coatings with different bias voltages is shown in Fig. 3. When the negative bias voltage increases from −50 V to −200 V, the deposition rate of TiN decreases sharply from 12.2 nm/min to 8.34 nm/min, and then decreases slightly from 8.34 nm/min to 7.8 nm/min with the further increase of bias voltage to −400 V. This may be related with the re-sputtering of the deposited coating caused by the heavy energetic ion bombardment[18]. Increasing negative bias voltage, the ions bombardment increases and as a consequence the growth rate increases. However, when the sputtering yield of Ti target is maximum, further increasing bias results in the heavy ion bombardment occurring in the surface of deposited coating, which are called the re-sputtered process, leading to the decrease of deposition rate of TiN coatings.

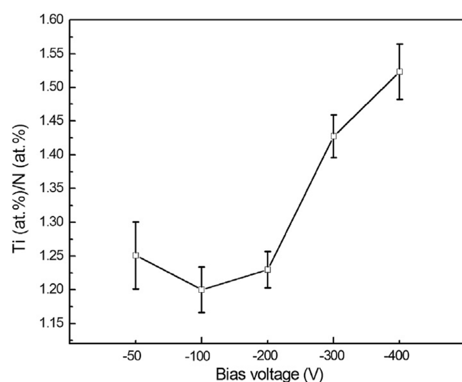

Fig. 4 Ti/N atomic ratio of the TiN coatings with different bias voltage.

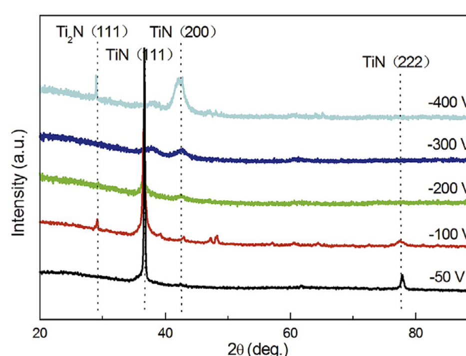

Fig. 5 XRD patterns of TiN coatings with different bias voltage.

Fig. 4 shows the chemical compositions of the TiN coatings. When the substrate bias voltage is less than −200 V, only a small change in Ti/N atomic ratio can be identified. However, it increases gradually as the bias voltage is varied from −200 V to −400 V. The enhanced ion bombardment during the deposition process can easily break the weak Ti−N bond and the N atoms are re-sputtered preferentially comparing with Ti ones.

Fig. 5 shows the XRD patterns of TiN coatings as a function of the substrate negative bias voltage. It is seen that the preferred orientation of TiN coating is shifted from (111) plane to (200) plane as the bias voltage increases from −50 V to −400 V. Similar changes in coating orientation have also been observed by varying the substrate negative bias in other reports[19,20]. Generally, this texture change in TiN coating is usually explained in thermodynamic and kinetic aspect. Thermodynamic consideration is proposed based on the minimization of total energy, which is the sum of surface energy and strain energy. Plane (111) and plane (200) have the lowest strain energy and the lowest surface energy in NaCl-type fcc nitrides, respectively[21]. Coatings deposited at low substrate bias preferring a (111) orientation for the highest number of atoms per unit area can be incorporated at low energy site. The increase in substrate bias increases the mobility of adatoms promoting the growth of lowest-surface-energy planes. A (200) texture is therefore expected to be the preferred orientation. From a kinetic aspect, if coatings are grown in relatively high-ion-energy conditions, their textures tend to evolve toward the planes with most open channels[22]. For the TiN coatings, (200) plane has opener channeling compared to (111) plane, the orientation changes from (111) to (200) plane as coatings are deposited under higher substrate bias. Meanwhile, the crystallite size of the TiN coating at (111) plane, which is determined from the Scherrer equation[23], tends to decrease from −50 V to −300 V as a result of the increased nucleation sites with the increase of incident ion energy[24] and followed by an increase as the substrate bias changes

Table 2 Grain size of the TiN coatings deposited at different negative bias voltage estimated from XRD analysis

Negative bias voltage (V)	Grain size (nm)
−50	38.1
−100	14.2
−200	8.6
−300	5.1
−400	7.7

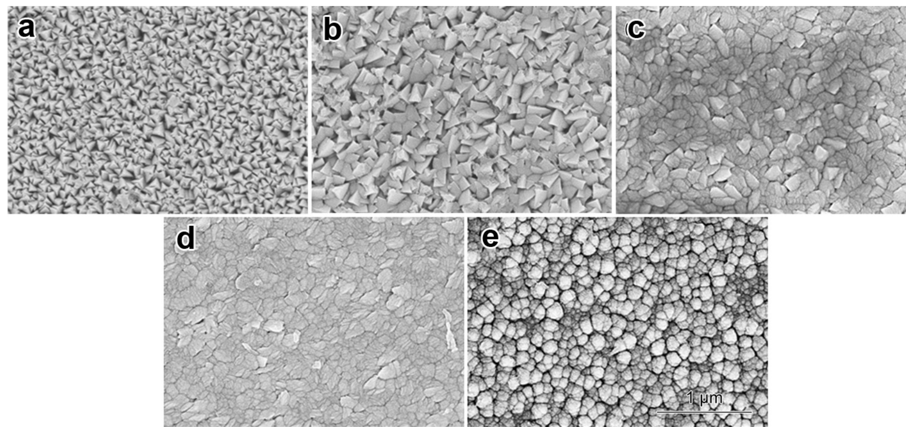

Fig. 6 Surface SEM images of the deposited TiN coatings with the bias voltage of: (a) −50 V, (b) −100 V, (c) −200 V, (d) −300 V, (e)−400 V.

from −300 V to −400 V because of high-energy ions bombardment, as illustrated in Table 2.

Fig. 6 shows surface morphologies of the deposited TiN coatings with different negative biases. It shows that TiN coatings exhibit the typical granular surface structure at the bias voltages from −50 V to −300 V. As the bias voltage increases to −400 V, a cauliflower-like structure appeared. This transition in coating surface structure could be attributed to the enhanced surface energy as the energy of incident ions increase[25]. Since the high ratio of ions to neutrons flux at higher bias voltage favors a higher surface mobility of adatoms, the shadowing effect is eliminated and the porosity fraction is reduced[26]. Therefore, the TiN coatings also exhibit a trend of densification. The cross-sectional images seen in Fig. 7 show that all the TiN coatings exhibit columnar-type structure. With increasing the negative bias voltage, the micrography evolves from the loose columnar structure to densely packed structure. The high mobility of the adatoms induced by ions bombardment with high incident energy is considered to modify the surface vacancies and diffuse among columns in the structure.

Fig. 8 shows the SPM images of the TiN coatings deposited at various bias voltages. It can be seen that the surface morphology of TiN coatings strongly depends on the bias voltage. A relatively flattened surface morphology is demonstrated at the bias voltage of −300 V. This difference in morphology is a consequence of the ion bombardment effects on surface mobility of tunable deposited atoms[27]. As shown in Fig. 8, the Ra value of TiN coatings decreases firstly and then increases. When the bias voltage is −300 V, the minimum Ra value of 10.05 nm is obtained, which is also confirmed by the SPM image. The increase of Ra value at the bias voltage of −400 V is caused by the extremely high-energy bombardment.

The hardness and Young's modulus of the TiN coatings with different bias voltages are shown in Fig. 9. The hardness and Young's modulus of TiN coating firstly increase and then decrease with increasing the bias voltage. At the bias of −300 V, The maximal values of hardness and elastic modulus are obtained at 17.4 ± 0.53 GPa and 263.8 ± 8.73 GPa, respectively. When the bias changes from −50 V to −300 V, the increase of hardness from 4.66 ± 0.18 GPa to 17.4 ± 0.53 GPa is attributed to the structure densification and the decreased crystallite size. At bias voltage of −400 V, the decrease of hardness and Young's modulus can be understood by the two factors. One is that the extremely high-energy ions bombardment induces higher temperature, which would promote crystallite size[24]. The other factor is that the Ti content in Ti_2N is higher than that in TiN phase, so the presence of Ti_2N (111) at the bias voltage of −400 V contributes to the decrease of the hardness and Young's modulus.

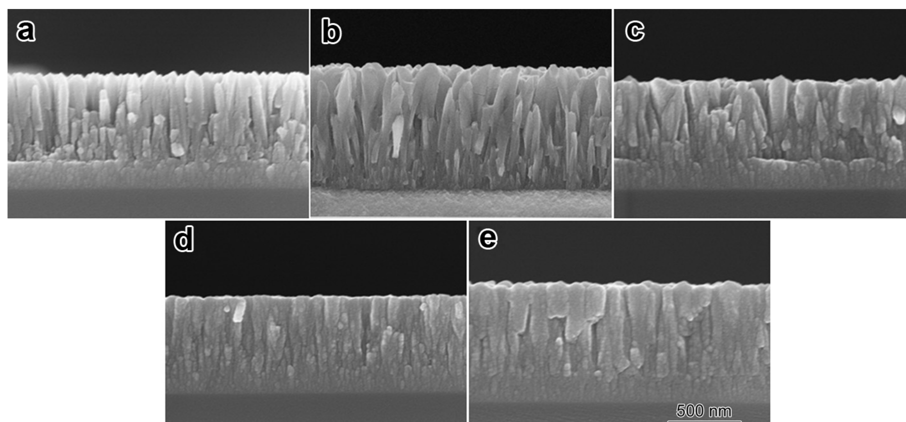

Fig. 7 Cross-section SEM images of the deposited TiN coatings with the bias voltage of: (a) −50 V, (b) −100 V, (c) −200 V, (d) −300 V, (e) −400 V.

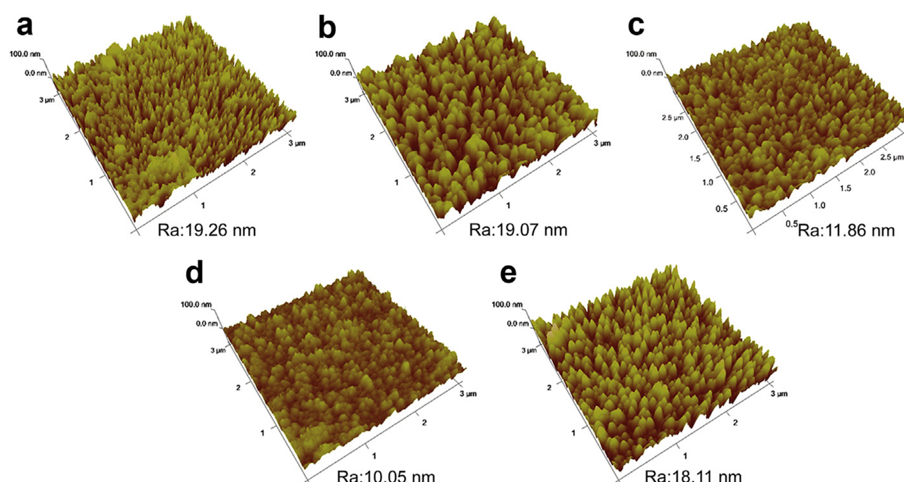

Fig. 8 SPM images of the coatings deposited at the bias voltage of: (a) −50 V, (b) −100 V, (c) −200 V, (d) −300 V, (e) −400 V.

The adhesion properties of TiN coatings are evaluated by the scratch tests. Fig. 10 shows the scratch track and the deduced critical loads of the coatings. With increasing the loads, the width and thickness of scratch track increase progressively until the critical loads (L_C), named by the mass delamination, happens in the coating. The lowest critical load is only about 1 N for the coatings deposited at −50 V, while the maximum critical load of 59 N is achieved at −300 V. Many researchers[28−30] have reported that the critical load increases linearly with the coatings hardness, which is consistent with our results. This general behavior has been explained in terms of the increasing load endurance of the coatings as its hardness increases. However, when the higher bias voltage was applied, the vertical cracks resulting from high-energy bombardments within the coatings and the lower hardness would deteriorate L_C to 40 N at −400 V.

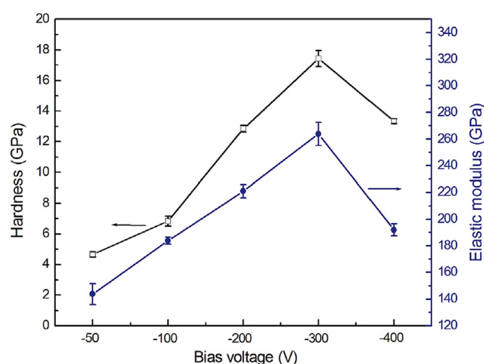

Fig. 9 Hardness and elastic modulus of the coatings as a function of bias voltage.

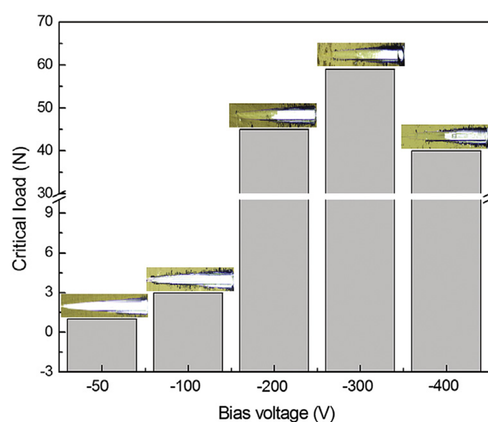

Fig. 10 The critical loads and the optical scratch images of the TiN coatings deposited on HSS at the bias voltage of: −50 V, −100 V, −200 V, −300 V, −400 V.

4. Conclusion

TiN coatings with the different negative bias voltages were deposited by a home-made HIPIMS technique. The evolutions of growth rate, composition, crystal structure and mechanical properties were studied systematically. It was found that increasing the bias voltage caused the decrease of deposition rate, accompanying with the structure densification and the decrease of surface roughness as expected. When the bias increased from −50 V to −300 V, the TiN coating gradually evolved from (111) orientation to (200) orientation, the hardness and Young's modulus firstly increased to 17.4 GPa and 263.8 GPa, respectively and then decreased with further increasing the bias. Similar result was observed in the changes of critical load as those of hardness evolution. In summary, the substrate negative bias voltage played a key role in the properties of the deposited TiN coatings due to the improved high ionization.

Acknowledgments

This work was financially supported by the program of National Natural Science Foundation of China (Grant No. 51375475) and the Instrument Developing Project of the Chinese Academy of Sciences (Grant No. YZ201326).

REFERENCES

[1] L.W. Ma, J.M. Cairney, M.J. Hoffman, P.R. Munroe, Surf. Coat. Technol. 204 (2010) 1764−1773.
[2] A. Yazdani, M. Soltanieh, H. Aghajani, S. Rastegari, Vacuum 86 (2011) 131−139.
[3] P.H. Mayrhofer, F. Kunc, J. Musil, C. Mitterer, Thin Solid Films 415 (2002) 151−159.

[4] P. Roquiny, A. Poulet, Y. Leys, J.C. Descamps, F. Bodart, P. VandenBrande, Thin Solid Films 355−356 (1999) 357−362.
[5] T. Matsue, T. Hanabusa, Y. Ikeuchi, Vacuum 74 (2004) 647−651.
[6] F.J. Jing, T.L. Yin, K. Yukimura, H. Sun, Y.X. Leng, N. Huang, Vacuum 86 (2012) 2114−2119.
[7] M. Hua, H.Y. Ma, J. Li, C.K. Mok, Surf. Coat. Technol. 200 (2006) 3612−3625.
[8] B. Window, N. Savvides, J. Vac. Sci. Technol. A 4 (1986) 196−202.
[9] R. Wei, E. Langa, C. Rincon, J. Arps, Surf. Coat. Technol. 201 (2006) 4453−4459.
[10] V. Kouznetsov, K. Macák, J.M. Schneider, U. Helmersson, I. Petrov, Surf. Coat. Technol. 122 (1999) 290−293.
[11] R. Chistyakov, B. Abraham, W.D. Sproul (Eds.), Proceedings of the 49th annual SVC technical conference, Washington, DC, April 23−27, 2006.
[12] L.J. Lin, W.D. Sproul, J.J. Moore, Z.L. Wu, S.L. Lee, R. Chistyakov, B. Abraham, JOM 63 (6) (2011) 48−58.
[13] A.P. Ehiasarian, R. New, W.D. Münz, L. Hultman, U. Helmersson, V. Kouznetsov, Vacuum 65 (2002) 147−154.
[14] X.P. Qin, P.L. Ke, A.Y. Wang, K.H. Kim, Surf. Coat. Technol. 228 (2013) 275−281.
[15] S. Gangopadhyay, R. Acharya, A.K. Chattopadhyay, S. Paul, Surf. Coat. Technol. 203 (2009) 1565−1572.
[16] X.B. Tian, Z.Z. Wu, J. Shi, X. Li, C. Gong, S.Q. Yang, Chin. Vac. 47 (2010) 44−47.
[17] A.P. Ehiasarian, A. Vetushka, A. Hecimovic, S. Konstantinidis, J. Appl. Phys. 104 (2008) 083305.
[18] M.K. Lee, H.S. Kang, J. Mater. Res. 12 (1997) 2393−2400.
[19] J.E. Greene, J.E. Sundgren, L. Hultman, I. Petrov, D.B. Bergstrom, Appl. Phys. Lett. 67 (1995) 2928−2930.
[20] R. Chandra, D. Kaur, A.K. Chawla, N. Phinichka, Z.H. Barber, Mater. Sci. Eng. A 423 (2006) 111−115.
[21] J. Pelleg, L.Z. Zevin, S. Lungo, N. Croitoru, Thin Solid Films 197 (1991) 117−128.
[22] W.J. Shen, M.H. Tsai, Y.S. Chang, J.W. Yeh, Thin Solid Films 520 (2012) 6183−6188.
[23] V. Uvarov, I. Popov, Mater. Charact. 58 (2007) 883−891.
[24] J.W. Lee, S.K. Tien, Y.C. Kuo, Thin Solid Films 494 (2006) 161−167.
[25] Y.P. Sharkeev, B.P. Gritsenko, S.V. Fortuna, A.J. Perry, Vacuum 52 (1999) 247−254.
[26] J.M. Poitevin, G. Lemperiere, J. Tardy, Thin Solid Films 97 (1982) 69−77.
[27] T. Takahashi, K. Masugata, H. Kawai, S. Kontani, J. Yamamoto, Vacuum 59 (2000) 777−784.
[28] A.J. Perry, Thin Solid Films 107 (1983) 167−180.
[29] P.A. Steinmann, H.E. Hintermann, J. Vac. Sci. Technol. A 3 (1985) 2394−2400.
[30] H. Ichimura, A. Rodrigo, Surf. Coat. Technol. 126 (2000) 152−158.